Atomic geometry, electronic states and bonding at the GaP(11)-Sb(1 ML) interface

1993 J. Phys.: Condens. Matter 5 4695

(http://iopscience.iop.org/0953-8984/5/27/014)

J. Phys.: Condens. Matter 5 (1993) 4695–4710. Printed in the UK

Atomic geometry, electronic states and bonding at the GaP (110)–Sb (1 ML) interface

G P Srivastava

Semiconductor Physics Group, Physics Department, University of Exeter, Stocker Road, Exeter EX4 4QL, UK

Received 2 March 1993

Abstract. We present a detailed investigation of the atomic geometry, electronic states and bonding of an ordered monolayer of Sb on the GaP(110) surface by using a first-principles pseudopotential method. It is found that the *epitaxially continued layer* structure is decisively more stable than the *relaxed* p^3, *epitaxial on top*, and *epitaxial overlapping chain* structures. The equilibrium geometry is characterized by a very small vertical shear between the Sb atoms and agrees well with measurements reported from the x-ray standing wave and surface extended x-ray-absorption fine-structure techniques. The calculated energy location and dispersion of the highest-lying occupied interface state compare very well with reported angle resolved photoemission studies. A thorough analysis of the nature of bonding between the overlayer and the substrate is provided. Finally the location and nature of the interface Fermi level pinning is discussed.

1. Introduction

The ordered growth of a monolayer of Sb on III–V (110) surfaces (Stringer *et al* 1983, Joyce *et al* 1990) provides a prototypical metal/semiconductor Schottky barrier system. Such a system is important for the development of sophisticated electronic devices. Apart from this importance, such an interface also provides an interesting system with usually very different physics than that of bulk or the clean surface of the semiconductor. The interaction between the metal (or semi-metal) and the semiconductor leads to atomic relaxation at the interface and results in new chemical bonds, thus giving rise to various localized electron states in different band gaps of the semiconductor.

The energy locations and dispersions of such states are sensitive functions of the atomic configuration at the interface. Therefore, in order to study the physics of metal/semiconductor interfaces, it is essential to determine the equilibrium atomic geometry. For the ordered (1 × 1) growth of a monolayer (1 ML) of Sb on III–V (110) surfaces four minimum-energy interface structures have been identified (LaFemina *et al* 1990). These are: Goddard's *epitaxially continued layer structure* (ECLS) (Swarts *et al* 1982), the relaxed Skeath or *relaxed* p^3 *structure* (Skeath *et al* 1983, Ford *et al* 1990), *epitaxial on top structure* (EOTS), and *epitaxial overlapping chain structure* (EOCS). The fourth structure was discarded by LaFemina *et al* on the grounds of increased interbond Coulomb repulsion and its incompatibility with the experimental low energy electron diffraction (LEED), scanning tunnelling microscopy (STM) and angle-resolved photoemission data for Sb/GaAs(110). Although recent LEED (Ford *et al* 1990 1992), x-ray standing wave (XSW) (Miyano *et al* 1992, Kendelewicz *et al* 1992), and surface extended x-ray-absorption fine-structure (SEXAFS) (Miyano *et al* 1993) studies have strongly supported the ECLS model, the recent

0953-8984/93/274695+16$07.50

theoretical work (LaFemina *et al* 1990) has been unable to discriminate between the first three geometries within the intrinsic accuracy of the empirical tight-binding method. STM micrographs have also been satisfactorily interpreted using these three geometrical models (Mårtensson *et al* 1988 1989). Likewise, photoemission data have been found to be in good agreement with the electronic states for both geometries calculated from the empirical tight-binding method (LaFemina *et al* 1990). Very few *ab initio* theoretical studies of such interfaces have been reported. In particular, available self-consistent calculations have either used LEED geometries (Bertoni *et al* 1983, Srivastava and Martin 1992) or geometries derived from the empirical tight-binding method (Manghi *et al* 1987). Thus our present understanding of the atomic structure and electronic states at the Sb/III–V (110) interface is far from being satisfactory.

In section 2 of this work we describe our theoretical method and its application to clean and covered (110) zinc blende surfaces. In section 3 we present our results for the atomic structure and electronic states on the clean GaP(110) surface and at the GaP(110)-Sb(1 ML) interface. Using the methods of total energy and forces we discriminate between the ECLS, p^3, EOTS and EOCS models for this interface. We further discuss the nature of bonding between the overlayer and the substrate, and the role of localized states in pinning the interface Fermi level in the bulk band gap. Finally some conclusions are drawn in section 4.

2. Theoretical method

An *ab initio* approach for the study of atomic geometry and electronic states at a surface or a metal/semiconductor interface requires (i) electron–ion potential energy obtained from first principles, (ii) a fundamental but practical scheme for electron–electron interaction, and (iii) an accurate and efficient numerical scheme for solving the appropriate quantum mechanical problem.

An excellent review of the theoretical method of Car and Parrinello (1985) has recently been presented by Payne *et al* (1992). In the molecular dynamics–density functional (MD–DF) scheme one considers a fictitious dynamical system whose Lagrangian is constructed in a configuration space spanned by the ionic coordinates $\{\boldsymbol{R}_I\}$ and the single-particle orbitals $\{\phi_i(\boldsymbol{r})\}$ of the DF theory. If μ is an adjustable parameter appropriate for the fictitious single-particle (electronic) dynamics, M_I denotes ionic masses, λ_{ij} are Lagrange multipliers used to satisfy the orthonormality of the ϕ_i, and $E(\{\boldsymbol{R}_I\}, \{\phi_i\})$ acts as the potential energy of the fictitious dynamical system, then using generalized coordinates $q = \{\boldsymbol{R}_I, \phi_I\}$ and generalized velocities $\dot{q} = \{\dot{\boldsymbol{R}}_I, \dot{\phi}_i\}$ the Lagrangian is expressed as†

$$L(q, \dot{q}) = \frac{\mu}{2} \sum_i \int d\boldsymbol{r} |\dot{\phi}_i|^2 + \frac{1}{2} \sum_I M_I \dot{\boldsymbol{R}}_I^2 - E[\{\boldsymbol{R}_I\}, \{\phi_i\}] + \sum_{i,j} \lambda_{ij} \left(\int d\boldsymbol{r} \phi_i^* \phi_j - \delta_{ij} \right). \tag{1}$$

The minimum of E with respect to the single-particle degrees of freedom $\{\phi_i\}$ is the Born–Oppenheimer potential $\mathcal{U}$ for the ions:

$$\mathcal{U}(\{\boldsymbol{R}_I\}) = \min_{\{\phi_i\}} E[\{\boldsymbol{R}_I\}, \{\phi_i\}]. \tag{2}$$

† For metallic systems occupation numbers $\{f_i\}$ of eigenvalues should be included as independent variables in addition to the orbitals $\{\phi_i\}$ (Yamamoto and Fujiwara 1992), but we do not consider this in the present study of semiconducting systems.

The simultaneous relaxation of the ionic and electronic coordinates towards their equilibrium on the Born–Oppenheimer surface is achieved by solving the Lagrange equations of motion

$$\frac{\mathrm{d}}{\mathrm{d}t}\frac{\partial L}{\partial \dot{q}} = \frac{\partial L}{\partial q}. \tag{3}$$

With (1) this yields

$$\mu\ddot{\phi}_i = -\frac{\delta E}{\delta \phi_i^*} + \sum_j \lambda_{ij}\phi_j = -H\phi_i + \sum_j \lambda_{ij}\phi_j \tag{4}$$

$$M_I\ddot{\boldsymbol{R}}_I = -\frac{\partial E}{\partial \boldsymbol{R}_I}. \tag{5}$$

In (4) H is the Hamiltonian of the electronic system, which in the DF theory is the Kohn–Sham Hamiltonian $H[\rho(\boldsymbol{r})]$, with $\rho(\boldsymbol{r}) = \sum_i \phi_i^*\phi_i$ as the electronic charge density (Srivastava and Weaire 1987). In the electronic ground state $\ddot{\phi}_i = 0$ and (4) reduces to the Kohn–Sham eigenvalue equation $H\phi_i = \varepsilon_i\phi_i$, with λ_{ij} replaced by the energy eigenvalues ε_i of state i.

Equations (4) and (5) can in principle be solved by several numerical techniques. In our work we solved the electronic equations of motion in (4) by using the scheme of Payne *et al* (1986), and the ionic equations of motion in (5) by using a damped steepest-descent method, as detailed below.

We considered an artificially defined periodic geometry along the surface normal. Each unit cell included eight atomic layers of the substrate semiconductor GaP, a single monolayer of the overlayer Sb on each side of the substrate slab, and a vacuum region equivalent of six substrate atomic layers. The electron–ion interaction was considered in the form of fully separable norm-conserving *ab initio* pseudopotentials (Kleinman and Bylander 1982, Gonze *et al* 1991). The many-body electron–electron interaction was considered within the local density approximation of the DF theory (Hohenberg and Kohn 1964, Kohn and Sham 1965), with the correlation scheme of Ceperley and Alder (1980) as parametrized by Perdew and Zunger (1981).

The single-particle orbitals $\{\phi_n\}$ were expanded in plane waves:

$$\phi_n(\boldsymbol{k}, \boldsymbol{r}) = \frac{1}{\sqrt{N_0\Omega}\sum_G b_{n,k+G}\exp[\mathrm{i}(\boldsymbol{k}+\boldsymbol{G})\cdot\boldsymbol{r}]} \tag{6}$$

with the system considered as N_0 unit cells each of volume Ω, $\boldsymbol{G}$ representing a reciprocal lattice vector, and n representing the band index. For such a basis set (4) can be solved analytically (Payne *et al* 1986): with a time step Δt, the equation of motion for the coefficients $b_{n,k+G}$ becomes

$$b_{n,k+G}(t+\Delta t) = 2\cos[\omega(t+\Delta t)]b_{n,k+G}(t) - b_{n,k+G}(t-\Delta t) - \frac{2\{1-\cos[\omega(t+\Delta t)]\}}{\mu\omega^2}\sum_{G'\neq G} V(\boldsymbol{k}+\boldsymbol{G}, \boldsymbol{k}+\boldsymbol{G}')b_{n,k+G'}(t) \tag{7}$$

with

$$\mu\omega^2 = \frac{\hbar^2}{2m}(\boldsymbol{k}+\boldsymbol{G})^2 + V(\boldsymbol{G}=0) - \varepsilon_{n,k}. \tag{8}$$

In (7) and (8) $\varepsilon_{n,k}$ represents the eigenvalue in band n of an electron with wavevector k, and $V(k+G, k+G')$ is the Fourier transform of the effective Kohn–Sham potential (Srivastava and Weaire 1987).

In order to solve the ionic equations of motion in (5) we used a damped steepest-descent algorithm. Accordingly, a starting configuration was assumed and after n iterations for ionic moves new ionic positions were obtained as follows:

$$R_I^{(n+1)} = R_I^{(n)} + \beta F_I^{(n)} + \gamma \dot{R}_I^{(n)} \tag{9}$$

with F_I as the Hellmann–Feynman force on ion I, β as a measure of inverse force constant, and γ as a damping coefficient. Thus, relaxation of the system to the nearest local minimum was achieved.

In (6) we considered plane waves up to the kinetic energy cutoff of 15 Ryd. The required k-space integrations were performed by using four special k-points in the irreducible part of the surface Brillouin zone (Evarestov and Smirnov 1983). The integration time step for the equations of motion was taken to be 2.0 au, the fictitious mass μ was taken to be 33 au, the inverse force constant β was considered as 1 au, and the damping coefficient γ was set to 0.1 au. The calculations were carried until forces on all ions dropped below 0.01 eV Å^{-1}.

3. Results

3.1. The clean GaP(110) surface

The calculated equilibrium cubic lattice constant for bulk GaP is 5.36 Å, which is within 1.7% of the experimental value, and this value is used in the surface and interface calculations. In order to appreciate the role of Sb adatoms on the electronic properties of the interface, it is important first to examine the atomic geometry and electronic states on the clean GaP(110) surface. The surface geometry has been studied experimentally using the LEED method (Duke *et al* 1981, Kahn 1983). The angle-resolved photoemission method (van Laar *et al* 1977, Straub *et al* 1985, Solal *et al* 1984, Cerrina *et al* 1985, Riesterer *et al* 1987, Carstensen *et al* 1990), electron energy-loss spectroscopy (Nannarone *et al* 1989), and reflection spectroscopy (Berkovits *et al* 1987) have been used to study occupied and unoccupied surface energy states. Three self-consistent theoretical studies of this surface have been reported (Manghi *et al* 1981 1990, Alves *et al* 1991). The theoretical works of Manghi *et al* (1981 1990) used a semiempirical local pseudopotential, a small basis set, and the relaxed surface geometry as determined from LEED studies (Kahn 1983). The present work uses the same theoretical method as the one used by Alves *et al* and thus the results are very similar. Therefore we only briefly discuss the main results which are relevant to the present study of the overlayer system.

The surface Ga and P atoms relax towards a planar and a pyramidal geometry respectively, giving rise to a vertical shear of 0.58 Å between the surface atoms and a tilt of 27.6° for the surface plane. Relative to the bulk-extrapolated plane the mass-weighted vertical height of the top surface layer is (−0.21 Å) $\hat{z}$ (i.e. the surface is contracted towards the substrate). The corresponding result for the second surface layer is (+0.05 Å) $\hat{z}$. The LEED study of this surface did not reveal any evidence for second-layer relaxation, but measured the contraction of the top layer to be 0.1 ± 0.05 Å (Duke *et al* 1981). The calculated surface bond lengths are conserved with respect to the bulk value to within 3%, in agreement with results for the cleaved surface of other zinc blende materials (Ferraz and Srivastava 1986 1987, Srivastava 1992). Table 1 gives the calculated geometrical parameters

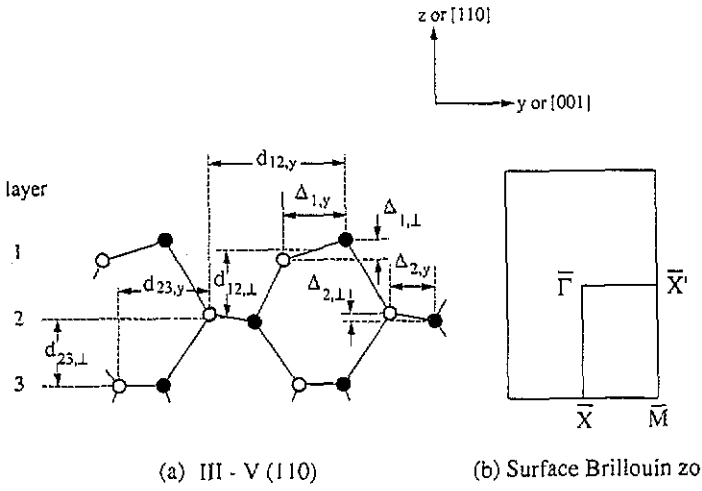

(a) III - V (110) (b) Surface Brillouin zone

Figure 1. Schematic side view of the relaxed III–V(110) surface. The tilt angle for the ith layer is defined as $\omega_i = \tan^{-1}(\Delta_{i,\perp}/\Delta_{i,y})$. A counterclockwise rotation from horizontal through the atoms in cation positions gives a positive angle. Also shown is the surface Brillouin zone.

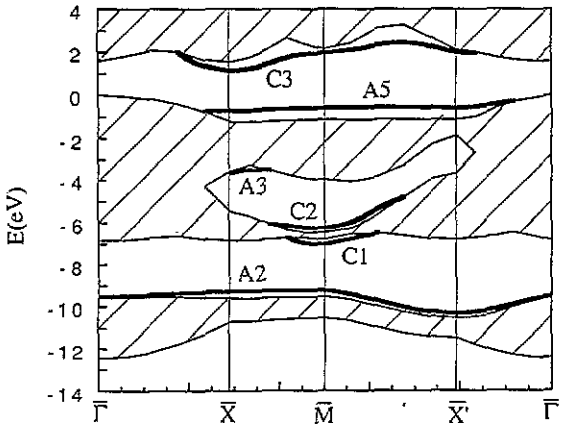

Figure 2. Electronic band structure of the GaP(110) surface. The hatched regions denote projected bulk bands, and the thick full curves show states localized on the surface layers.

shown in figure 1 where a sign convention for surface tilt angle has also been defined. The computed surface band structure is shown in figure 2. In general there is agreement between computed and experimentally measured surface-state energies, as discussed in the work of Alves *et al* . The states A2, C2, A5 and C3 are localized on the first layer cation (C) and anion (A) atoms, while the states C1 and A3 are localized on the second layer cation and anion atoms respectively. These features are common to the (110) surface of all zinc blende surfaces (Srivastava *et al* 1983, Ferraz and Srivastava 1986, Alves *et al* 1991). At $\bar{X}$ the state A5 lies at 0.75 eV below the top of the bulk valence band (E_v) of GaP and shows only a small dispersion along $\bar{X}$–$\bar{M}$–$\bar{X}'$ in the surface Brillouin zone. This energy location agrees very well with the photoemission measurement of 0.8 eV by Cerrina *et al* (1985). The minimum of the lowest unoccupied surface state C3 lies approximately 0.5 eV below the bulk conduction band minimum and is located at the $\bar{X}$ point. The theoretical location of C3 at 1.1 eV above E_v is consistent with the inverse photoemission measurement of 1.7 eV (van Laar *et al* 1977), remembering that we have used the local density approximation, which underestimates band gaps in semiconductors.

3.2. The GaP(110)–Sb(1 ML) interface

We studied the four local energy-minimum structures as mentioned in the introduction. The chemisorption energy has been calculated to be (4.51, 4.25, 4.13, 3.45) eV per adatom for the optimized (ECLS, EOTS, p^3, EOCS) geometry. Clearly the binding energy between the Sb overlayer and the GaP substrate for the EOCS is much too low compared to that for the other three structures. For this reason the EOCS structure has not been discussed further in this work.

In this section we discuss the atomic geometry, localized electron states and the nature of bonding at the Sb/GaP(110) interface. Although the ECLS model gives the lowest energy configuration, we also present results for the p^3 and EOTS models.

3.2.1. Atomic geometry. The structural parameters for the ECLS, p^3 and EOTS models are defined in figure 3. Our first interest is to study these structural parameters and their variation among the three competing geometrical models. The results are given in table 1, and are discussed below.

Table 1. Structural parameters for the equilibrium geometries of the clean GaP(110) surface and the GaP(110)–Sb(1 ML) interface. The sign convention for angles is explained in the caption for figure 1. C_i and A_i represent, respectively, atoms in the cation and anion positions in the ith layer.

System	$\Delta_{1,\perp}$ (Å)	ω_1 (deg)	$\Delta_{2,\perp}$ (Å)	ω_2 (deg)	$d_{12,\perp}$ (Å)	C_1–A_1 (Å)	C_1–A_2 (Å)	A_1–C_2 (Å)	C_2–A_2 (Å)
GaP(110)									
Present work	0.58	27.6	0.08	−3.17	1.63	2.26	2.35	2.25	2.32
LEED[a]	0.63	27.5	0.08						
Sb/GaP(110)									
Present work									
ECLS	0.05	1.43	0.03	−1.38	2.36	2.77	2.57	2.55	2.32
EOTS	0.10	−2.63	0.07	−3.13	2.56	2.82	2.57	2.62	2.30
p^3	0.56	15.7	0.18	7.46	2.35	2.81	2.67	2.70	2.32
XSW[b]	0.04 ±0.1				2.31 ±0.1				
SEXAFS[c]						2.88	2.60	2.79	

[a] Duke *et al* (1981), Kahn (1983).
[b] Miyano *et al* (1992).
[c] Miyano *et al* (1993).

The Sb overlayer on the GaP(110) is characterized by a vertical shear of (0.05 Å, 0.56 Å, 0.10 Å) and a tilt angle of (1.43°, 15.7°, −2.63°) for the (ECLS, p^3, EOTS) model. The top substrate (GaP) layer has a vertical shear of (0.03 Å, 0.18 Å, 0.07 Å) and a tilt angle of (−1.38°, 7.46°, −3.13°) for the (ECLS, p^3, EOTS) model. The sign convention for the tilt angle is the same as explained in the caption for figure 1. The Sb–Sb and Ga–P bond lengths are nearly identical for the three geometries. The overlayer–substrate bond lengths Sb–P (C_1–A_2) and Sb–Ga (A_1–C_2) for the p^3 structure are 3–5% larger than those for the ECLS and EOTS. The vertical height of the Sb chain above the top substrate layer ($d_{12,\perp}$) is calculated to be (2.36 Å, 2.35 Å, 2.56 Å) for the (ECLS, p^3, EOTS) model. From the above results it is clear that the structural parameters for the three competing models are appreciably different. Whereas for the ECLS and EOTS models the substrate GaP layer has acquired a small counter-relaxation and the vertical shear between the Sb adatoms is

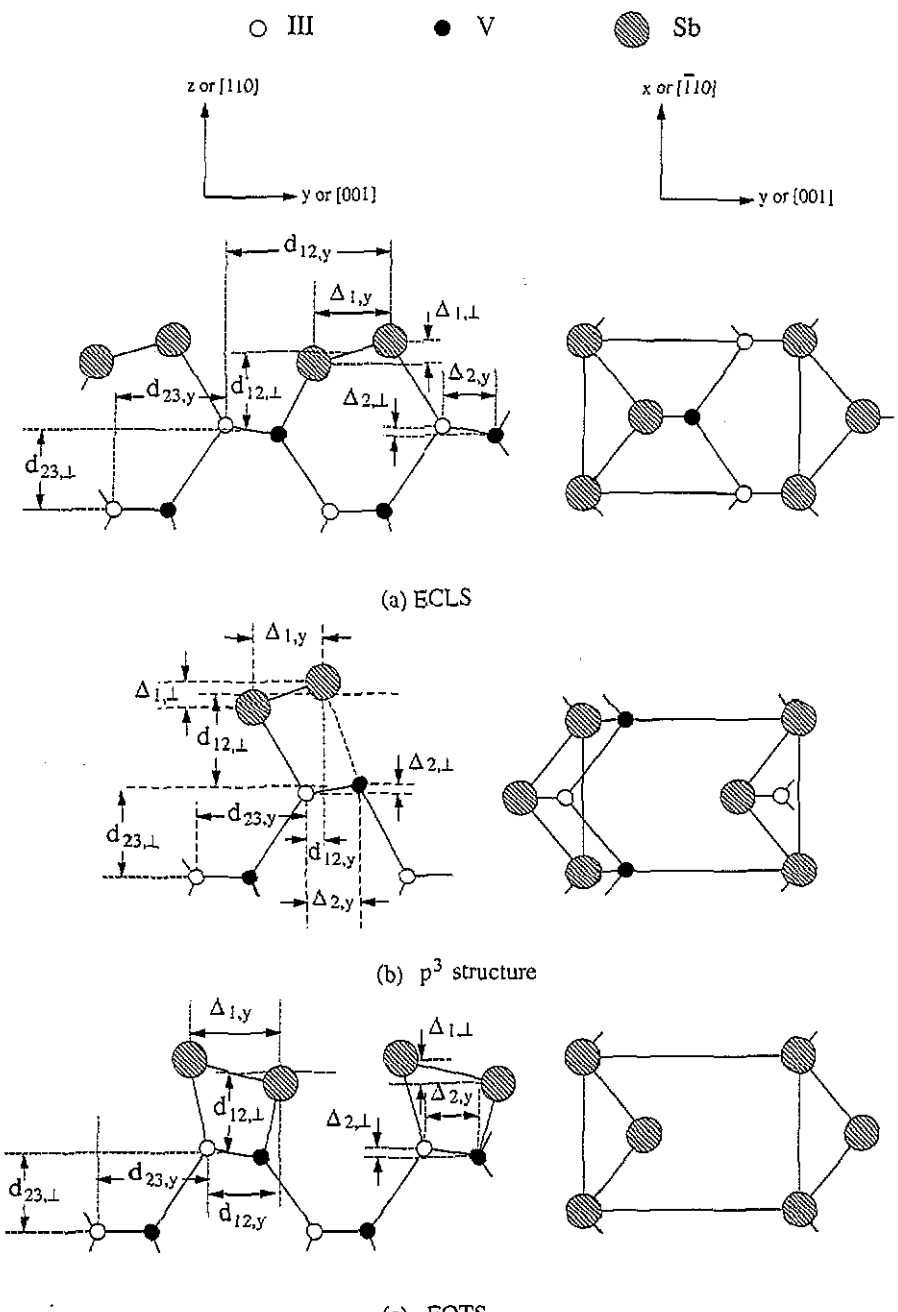

Figure 3. Schematic side and top views of the relaxed III–V (110)-Sb(1 ML) interface in the ECLS, p^3 and EOTS models. The sign convention for layer tilt angles is explained in figure 1.

negligible, for the relaxed Skeath (p^3) model the substrate remains significantly relaxed and there exists a large vertical shear between the Sb atoms. Although the Sb atom bonded to the Ga atom lies slightly further away from the substrate for both the ECLS and EOTS, these two models can be discriminated against each other: (i) the vertical distance between the

overlayer and the substrate ($d_{12,\perp}$) for the EOTS model is 8.5% larger than that for the ECLS model, and (ii) relative to the bulk-extrapolated plane the substrate layer is contracted by 0.13 Å (0.23 Å) for the ECLS (EOTS) model.

From our work we observe that the bond lengths at the interface show the trend $d_{Sb-Sb} > d_{Ga-Sb} \geqslant d_{Sb-P} > d_{Ga-P}$ for each of the ECLS, p^3 and EOTS models. We find that within about 1.5% the Sb–Sb bond length remains the same at Sb/GaP(110) for each of the ECLS, p^3 and EOTS models, and also at Sb/GaAs(110) and Sb/InP(110) for the ECLS model (Srivastava 1992). Within a few per cent of the bond lengths d_{Ga-Sb} and d_{Sb-P} the calculated trend is similar to that obtained by using the tetrahedral radii of Ga, P and Sb (Burns 1985). Thus our prediction of the trend in the bond lengths provides a firm support to the hypothesis of Duke *et al* (1982) that surface bond lengths on both clean and adsorbate-overlayer systems are compatible with the simple concept of conservation of Pauling's covalent radii (Pauling 1967).

Our calculated geometrical results can be compared with the recent measurements made by using the XSW (Miyano *et al* 1992) and SEXAFS (Miyano *et al* 1993) techniques. From the XSW study Miyano *et al* measured the perpendicular distance of the Sb chain from the bulk-extrapolated (220) plane to be 2.31 ± 0.10 Å. They concluded that this value should represent the displacement of the Sb chain from the GaP surface layer to within the quoted uncertainty. This measured estimate compares well with our calculation of the average vertical distance between the Sb chain and the GaP surface layer, $d_{12,\perp}$, for the ECLS and p^3 models, but not for the EOTS model. On the other hand, the XSW-measured vertical shear $\Delta_{1,\perp} = 0.04 \pm 0.1$ Å of the Sb chain compares well with our calculation for the ECLS and EOTS models, but not the p^3 model. The calculated vertical shear $\Delta_{1,\perp} = 0.56$ Å for the p^3 model lies well beyond the bounds quoted in the XSW measurements. Similar to the XSW study, the polarization dependence of SEXAFS measurements by Miyano *et al* (1993) rules out any tilted-chain (e.g. p^3 or EOCS) for this interface. The SEXAFS study also rules out the EOCS model on the basis of the measured coordination numbers of the first-shell neighbours to the overlayer Sb atoms. From a combination of the XSW and SEXAFS measurements Miyano *et al* (1993) deduce, with a relatively large degree of uncertainty, that in the ECLS model the adsorption of Sb would result in a contraction of the GaP surface layer by the amount 0.19 ± 0.15 Å. From our work we find that the contraction of the GaP layer is (0.13 Å, 0.16 Å, 0.23 Å) for the (ECLS, p^3, EOTS) models.

As SEXAFS studies provide a direct measurement of adatom-substrate and adatom-adatom bond lengths, it is particularly interesting to directly compare our theoretically calculated bond lengths with SEXAFS-derived bond lengths. From table 1 it can be seen that our calculated values of d_{Sb-P} for the three models compare very well with the SEXAFS result. Similarly, the theoretical values of d_{Sb-Sb} for the three models compare well with the SEXAFS result within the limits of theoretical and experimental accuracies. However, the theoretical value of d_{Ga-Sb} compares reasonably well with the SEXAFS result only for the p^3 model: the theoretical result for the ECLS (EOTS) being 8.5% (5%) smaller than the SEXAFS result. It is interesting to note that in an earlier work on Sb/GaAs(110) (Srivastava 1992) we calculated $d_{Ga-Sb} = 2.59$ Å for the ECLS, a result almost identical to the one given in table 1. Therefore the source of discrepancy between theory and experiment regarding the value of d_{Ga-Sb} remains unclear. From the above discussion it is clear that the best overall structural agreement between theory and experiment exists only for the ECLS model.

At present there are no LEED results available for the structural characterization of Sb/GaP(110). However, our calculated structural parameters for Sb/GaP(110) for both the ECLS and p^3 models are in their respective ranges of values determined by recent LEED analyses of Sb/GaAs(110) and Sb/InP(110) (Ford *et al* 1990, 1992). Thus we may

conclude that a LEED analysis would produce structural parameters for Sb/GaP(110) in close agreement with our predictions.

Previous theoretical determination of the structural parameters for Sb/GaP(110) employed an empirical tight-binding method (Mailhiot *et al* 1985, LaFemina *et al* 1990). The two estimates of $\Delta_{1,\perp}$ for the ECLS geometry disagree significantly, but the smaller of the two values presented in the more recent work is quite comparable to our prediction. Similarly, the results given in the two works for the tilt angle of the overlayer also differ significantly, with the recent result being closer, but still much larger, than ours. For the EOTS geometry LaFemina *et al* have calculated the shear of the overlayer to be 0.16 Å, a result which is quite close to our prediction of 0.10 Å. Their calculated tilt angle for the overlayer in the EOTS is 4.8°, also a result similar to our prediction. However, their work predicts that the *average* vertical distance $d_{12,\perp}$ for the EOTS is about 0.33 Å bigger than that for the ECLS while our work predicts this difference to be only 0.2 Å. Such a discrepancy between the results of LaFemina and ours is not surprising, because while our *ab initio* work predicts structural parameters which are accurate to within ±0.03 Å, the uncertainty in the predictions using the empirical approaches of both Mailhiot *et al* and LaFemina *et al* is ±0.2 Å.

LaFemina *et al* calculated the total energy of the ECLS geometry to be approximately 0.19 eV per adatom per unit cell lower than that of the EOTS geometry. However, it should be pointed out that within the intrinsic accuracy of their theoretical scheme these workers were unable to clearly distinguish between the relative stability of the two structures. Our work decisively favours the ECLS model over the EOTS and p^3 models, with a gain respectively of 0.26 and 0.38 eV per adatom per unit cell. The large energy gain for the ECLS over the p^3 structure comes largely from the lowering of the potential energy in the former model with the Sb atoms pointing closely along the dangling bonds of the substrate atoms.

Finally, we note that Mailhiot *et al* attempted to correlate the magnitude of the vertical shear $\Delta_{1,\perp}$ between the two inequivalent Sb atoms with two separate phenomena: the geometrical and electronic inequivalence of the anions and cations in the substrate. In figure 4(*a*) and (*b*) we have plotted such variations for the ECLS using our results for the Sb overlayer on the (110) surface of GaP (present work), and GaAs and InP (Srivastava 1992). Although there is no clearly definable trend, it can be said that both the trends seen in the work of Mailhiot *et al* namely that $\Delta_{1,\perp}$ decreases with increase in the Sb-substrate–anion bond length and increases with increase in the spectroscopic ionicity (Phillips 1970) of the substrate, are supported by our work.

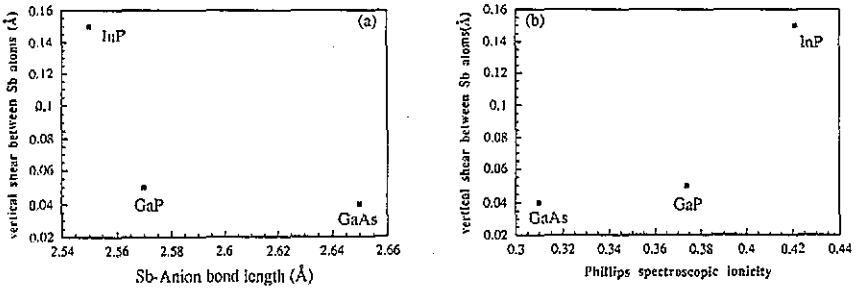

Figure 4. (*a*) The vertical shear between Sb atoms, $\Delta_{1,\perp}$, plotted as a function of the Sb–anion bond length for an ordered monolayer growth of Sb on the (110) surface of GaAs, GaP and InP. (*b*) $\Delta_{1,\perp}$ plotted against Phillips' spectroscopic ionicity of the substrate.

3.2.2. Localized electron states. The calculated electronic states for the ECLS, p^3 and EOTS models of Sb/GaP(110) are found to be unambiguously distinct, both in energy location and dispersion, but only for the states lying in the fundamental band gap of bulk GaP. In general we have identified a total of seven occupied and two lowest unoccupied electron states which are localized at the interface. The occupied states have been denoted S1–S5, C′ and A′, and the unoccupied states have been labelled S6 and S7 (figure 5(*a*)–(*c*)). We will discuss their orbital character in the following subsection.

The states S1 and S2 are found to lie in the ionicity gap of GaP, and both show similar energy location and dispersion for the ECLS, p^3 and EOTS models. The states C′ and S3 lie in the stomach gap of GaP, and again their energy location and dispersion are generally similar for both the geometries. A closer examination, however, reveals that the S3 state lies somewhat lower in energy for the p^3 and EOTS models than for the ECLS model. At the $\bar{X}'$ point this difference is approximately (0.15 eV, 0.35 eV) for the (p^3, EOTS) model.

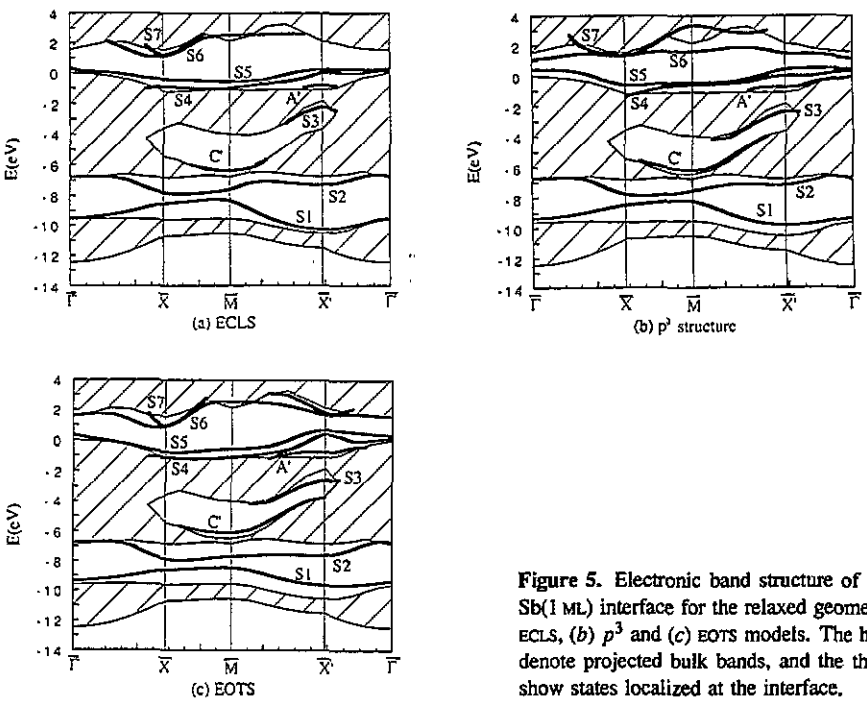

Figure 5. Electronic band structure of the GaP(110)-Sb(1 ML) interface for the relaxed geometries in the (*a*) ECLS, (*b*) p^3 and (*c*) EOTS models. The hatched regions denote projected bulk bands, and the thick full curves show states localized at the interface.

The clearest and most interesting difference between the electronic states for the ECLS, p^3 and EOTS models is exhibited by the occupied states A′, S4, and S5 , and the unoccupied state S6 lying in the fundamental band gap of GaP. The most noticeable difference occurs in the energy location and dispersion of the highest occupied state S5 and lowest unoccupied state S6. The state S5 has the least amount of dispersion for the ECLS model, and the state S6 has the least amount of dispersion for the p^3 model. With reference to the top of the bulk valence band edge (E_v) the bottom of S6 is at 1.0 eV located at 0.8$\bar{\Gamma}\bar{X}$ for the ECLS, at 1.15 eV located at $\bar{\Gamma}$ for the p^3 structure, and 0.65 eV located at 0.8$\bar{\Gamma}\bar{X}$ for the EOTS. The top of S5 is located at $\bar{\Gamma}$ and lies at 0.31 eV for the ECLS, and at 0.45 eV for the p^3 structure, but is located at 0.8$\bar{M}\bar{X}'$ and lies at 0.65 eV for the EOTS. Thus while the ECLS and the p^3 models are semiconducting with band gaps 0.7 eV and 0.6 eV, respectively, the optimized EOTS model is found to have a nearly zero band gap (between 0.8$\bar{\Gamma}\bar{X}$ and

$0.8\bar{M}\bar{X}'$). Although these values of the band gap are underestimated due to the application of the local density approximation, it is nevertheless very clear that the EOTS model can be easily discriminated from the ECLS and p^3 models.

To our knowledge so far there has been only one report of angle-resolved photoemission measurements on GaP(110)–Sb(1 ML) (Tulke and Lüth 1986). In figure 6 we compare our calculation of S5 along $\bar{\Gamma}$–$\bar{M}$ for the ECLS, p^3 and EOTS models with the photoemission data. Clearly the result for the p^3 model is the least favourable to the experiment. In particular, the location of this state at $\bar{\Gamma}$ and $\bar{M}$, together with the amount of dispersion between the two points, is in better agreement with the experiment for the ECLS and EOTS models.

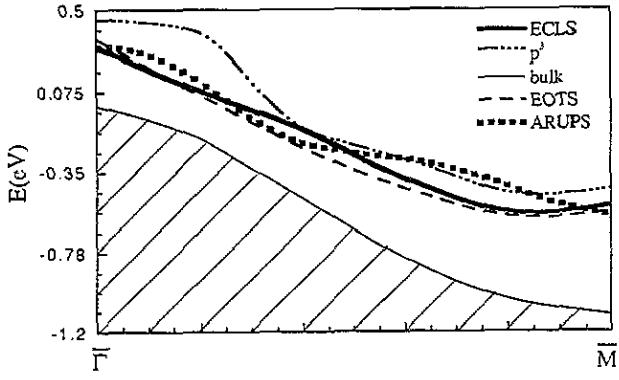

Figure 6. Energy location and dispersion along $\bar{\Gamma}$–$\bar{M}$ of the highest-lying occupied interface state S5 for the ECLS, p^3 and EOTS models of GaP(110)–Sb(1 ML). The results for the ECLS and EOTS are in better agreement with the angle-resolved photoemission data of Tulke and Lüth.

3.2.3. Nature of bonding. On account of the lowest-energy configuration, and on the basis of the comparison of our results with the XSW, SEXAFS and angle-resolved photoemission measurements, we consider ECLS to be the correct model for the GaP(110)–Sb(1 ML) interface. It is therefore the only model discussed further in this work. Now we discuss the nature of bonding at this interface from an analysis of the charge density plots shown in figures 7 and 8. The first observation we make is that the two inequivalent Sb atoms in the unit cell behave differently. The Ga–Sb bond is similar to that observed in GaSb semiconductor. The Sb atom bonded to P behaves more like a group III atom. This is consistent with the fact that P is more electronegative than Sb. The total charge density has a larger maximum along Sb–P than along Ga–Sb, indicating that despite being nearly equal in length the former bond is stronger than the latter. The p_z orbitals of neighbouring atoms in the Sb chain combine to produce a π bonding as is clearly seen in figure 7(*c*). A thorough analysis of the electronic charge density for individual bands reveals that the localized states at this interface fall into three groups. No attempt was made to identify resonant interface states, which may show orbital characters different from those discussed in this work.

States localized on the overlayer.
The states S1 and S2 are s-like and have very strong localization on the overlayer Sb atoms, with a small hint of bonding with the s electrons of substrate Ga and P atoms, respectively. Therefore these can be classified as states truly localized on the overlayer.

States localized on the top substrate layer.
As we discussed in section 3.2.1 upon the deposition of Sb the top GaP layer is

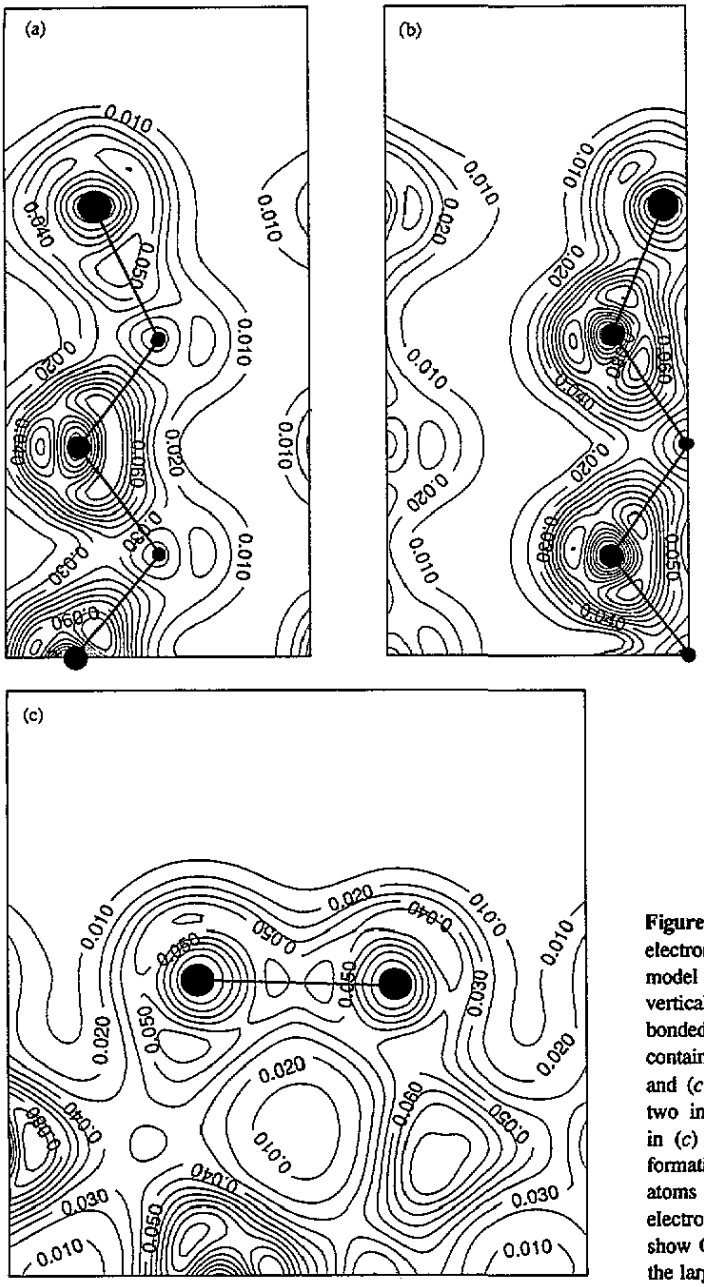

Figure 7. Contour plots of the total electronic charge density for the ECLS model of GaP(110)–Sb(1 ML) in (*a*) a vertical plane containing the Sb atom bonded to Ga, (*b*) a vertical plane containing the Sb atom bonded to P, and (*c*) a vertical plane containing the two inequivalent Sb atoms. The plot in (*c*) clearly shows a strong π bond formation between the two inequivalent atoms in the Sb chain. The units are electrons bohr^{-3}. Small and big dots show Ga and P atoms respectively, and the large shaded circles show Sb atoms.

greatly derelaxed, and the second substrate layer now behaves almost like the bulk layer. Consequently the states C1 and A3 localized on the second layer of the clean GaP(110) surface have almost turned into bulk states and can no longer be clearly identified as localized. The top substrate layer now acts as the second layer of the new system (the interface system) and new states, C′ and A′, are induced by the growth of the overlayer which are localized on the top substrate layer. Lying in the bottom of the stomach gap C′ has an s character and is derived mainly from the Ga atom but also has a small contribution

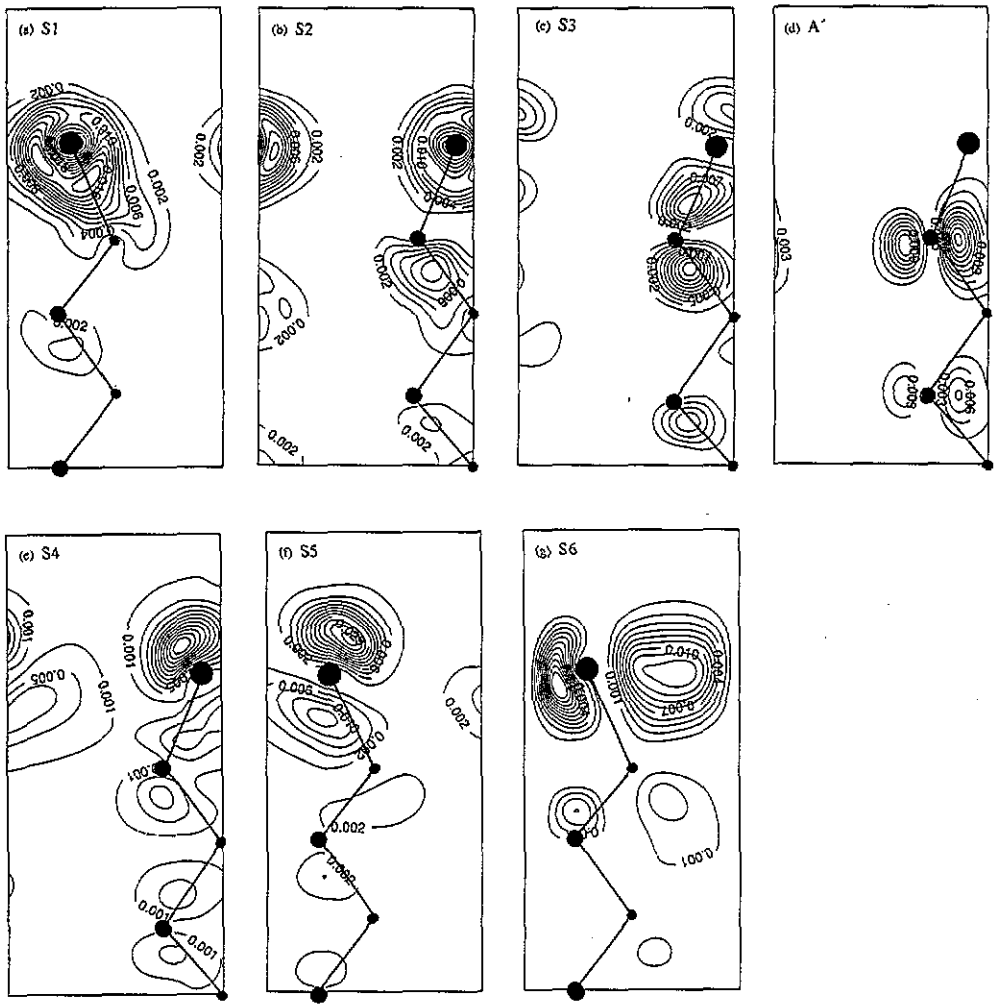

Figure 8. Contour plots of electronic charge density for individual states localized at the GaP(110)–Sb(1 ML) interface using planes (*a*) and (*b*) of figure 7. Shown are the states (*a*) S1 at $\bar{X}$, (*b*) S2 at $\bar{X}$, (*c*) S3 at $\bar{X}'$, (*d*) A' at $\bar{X}'$, (*e*) S4 at $\bar{X}$, (*f*) S5 at $\bar{X}$, (*g*) S6 at $\bar{X}$. Units are electrons bohr^{-3}. Small and big dots show Ga and P atoms respectively, and the large shaded circles show Sb atoms.

from the overlayer Sb atom. Localized at the P atom, A' has a p_y character and lies in the fundamental band gap just above the top of the valence band near $\bar{X}'$. The states C' and A' of the interface system therefore correspond to the states C1 and A3 of the clean surface. We also find that the energy location and dispersion of C' is almost identical to that of the state C1 on the clean surface.

Overlayer–substrate chemisorbed states

The third group of localized electron states arises due to chemical bonding between the overlayer Sb atoms and the top substrate layer Ga and P atoms. S3 is made up from a combination of the p_z orbitals of Sb and P and lies at the top of the stomach gap near $\bar{X}'$. The state S4 appears to have a bonding character between the P dangling sp^3 orbital and the Sb–Sb ppπ orbital. The highest occupied state, S5, appears to be due to bonding between

the Ga dangling sp^3 orbital and the Sb–Sb ppπ orbital. The lowest unoccupied state, S6, results from an antibonding combination of the Ga dangling sp^3 orbital and the Sb–Sb ppπ orbital.

The relative energy placement of the S4 and S5 states is consistent with the observation that on the clean surface the dangling bond states A5 and C3 lie near the bulk valence and conduction band edges, respectively, and that for the overlayer system S4 and S5 are replacements for A5 and C3, respectively.

Our description of the two highest occupied states, S4 and S5, and the lowest unoccupied state, S6, agrees very well with the corresponding states S_5, S_6 and S_7 in the work of Manghi *et al* (1987). However, due mainly to the rather inaccurate atomic geometry used by Manghi *et al* taken from the empirical tight-binding work of Mailhiot *et al* (1985), we are unable to identify many other of their states with ours. We feel that the energy placement and dispersion of some of the states, specially with large binding energies, presented in the work of Manghi *et al* would also significantly change with the choice of a larger basis set, thus bringing their results much closer to ours.

The comment made about the work of Manghi *et al* is also relevant to an earlier work of ours (Srivastava and Martin 1992). For the study of the InP(110)–Sb(1 ML) interface we used a small basis set and an earlier LEED geometry (Duke *et al* 1985) which is now known to be quite inaccurate (Srivastava 1992). Nevertheless, the nature of localization of at least some of the electron states studied in that work is similar to that obtained in this work. In particular, the states S4, S5 and S6 in this work can be identified, respectively, with the states S_9, S_7 and S_{11} in the work of Srivastava and Martin.

3.2.4. Implications for Schottky barrier formation. From the point of view of Schottky barrier formation at the interface studied in this work the most important role is played by the localized states S5 and S6 which arise from chemisorption between the (semi)metal Sb and the substrate. For a p-type substrate the Schottky barrier height is controlled by the state S5 which would pin the interface Fermi level. For an n-type substrate the state S6 controls the situation, with the energy difference between the bottom of the bulk conduction band (E_c) and S6 as a measure of the barrier height. It is therefore important to get an accurate estimate of the position of S6 relative to E_c. In this respect we remember that the present work is based on the application of the local density approximation which is principally valid for occupied states and results in an underestimation of the fundamental band gap in semiconductors. It should also be noted that the discussion relating to the band gap underestimation has in the literature been made with theoretical gaps calculated at experimental lattice constant. As mentioned earlier in this work we have used our theoretically determined lattice constant for GaP (approximately 1.7% smaller than the experimental value). This results in a band gap of 1.54 eV for GaP. It is expected that when a quasi-particle calculation is performed, the calculated band gap would be in a reasonable agreement with experiment. Most quasi-particle calculations, however, indicate that there is almost a constant shift throughout the Brillouin zone for both bulk conduction bands (Godby *et al* 1988, Jenkins *et al* 1993) as well as localized surface state energies (Zhu *et al* 1989). Assuming that both the bulk conduction band edge and the interface state S6 are altered by roughly the same amount, we would expect our calculated value E_c–E(S6) of approximately 0.5 eV for the ECLS to be a fair estimate for the Schottky barrier height at the n-GaP(110)–Sb(1 ML) interface.

From the soft x-ray photoemission spectroscopic data of Miyano *et al* (1990) the interface Fermi level for a monolayer coverage of Sb can be estimated to be approximately at 1.2 eV above the bulk valence band edge E_v. This result seems to agree very well with

the energy location of S6 in our work. However, as we have remarked above our estimate of $E(S6)$–E_v, obtained using the local density approximation, must be an underestimation. Therefore we suggest that the energy location of the interface Fermi level in the work of Miyano *et al* is somewhat lower than it ought to be. Indeed, this may be so because of the poor quality sample used in their work.

From the discussion presented earlier it is clear that the height and nature of the Schottky barrier at the n-GaP(110)–Sb(1 ML) is determined by the chemical bond formation between the substrate Ga atoms and the Sb chain. Only at coverages above one monolayer might the nature of the barrier be correlated to Sb-induced gap states (i.e. MIGS, as suggested by Heine (1965)) and eventually perhaps to a near-ideal Schottky-like behaviour as reported for metals on GaP by Brillson *et al* (1987).

4. Conclusions

We have presented a first-principles pseudopotential study of the ordered growth of a monolayer of Sb on the (110) surface of GaP. We have clearly ruled out the EOTS, p^3 and EOCS models in favour of the ECLS geometry on the basis of total-energy calculations. Deposition of an ordered monolayer of Sb almost completely removes the relaxation of the GaP surface layer, and the vertical shear between the Sb atoms is also very small. The chemisorption energy of the Sb overlayer is 4.51 eV per adatom. The ECLS model also produces the best overall comparison between our theoretical results and available XSW, SEXAFS, angle-resolved, and soft x-ray photoemission spectroscopic measurements. Finally, we have pointed out that the formation of Schottky barrier is influenced by Fermi level pinning at the n-GaP(110)–Sb(1 ML) interface, which in turn is attributed to a chemical bond formation between the substrate Ga atoms and the overlayer Sb chain.

Acknowledgments

It is a pleasure to thank Professor M Scheffler and Mr R Stumpf for many stimulating discussions on the application of the molecular dynamics method. This work has been supported by the SERC, UK.

References

Alves J L A, Hebenstreit J and Scheffler M 1991 *Phys. Rev.* B **44** 6188
Berkovits V L, Ivantsov L F, Makarenko I V, Minashvili T A and Safarov V I 1987 *Solid State Commun.* **64** 767
Bertoni C M, Calandra C, Manghi F and Molinari E 1983 *Phys. Rev.* B **27** 1251
Brillson L J, Vituro R E, Slade M L, Chiaradia P, Kilday D, Kelley M K and Margaritondo G 1987 *Appl. Phys. Lett.* **50** 1379
Burns G 1985 *Solid State Physics* (New York: Academic)
Car R and Parrinello 1985 *Phys. Rev. Lett.* **55** 2471
Carstensen H, Claessen R, Manzke R and Skibowski M 1990 *Phys. Rev.* B **41** 9880
Ceperley D M and Alder B J 1980 *Phys. Rev. Lett.* **45** 566
Cerrina F, Bommannavar A, Benbow R A and Hurych Z 1985 *Phys. Rev.* B **31** 8314
Duke C B, Mailhiot C, Paton A, Li K, Bonapace C and Kahn A 1985 *Surf. Sci.* **163** 391
Duke C B, Paton A, Ford W K, Kahn A and Carelli J 1981 *Phys. Rev.* B **24** 562
—— 1982 *Phys. Rev.* B **26** 803
Evarestov R A and Smirnov V P 1983 *Phys. Stat. Solidi (b)* **119** 9
Ferraz A C and Srivastava 1986 *J. Phys. C: Solid State Phys.* **19** 5987

—— 1987 *Surf. Sci.* **182** 161
Ford W K, Guo T, Lessor D L and Duke C B 1990 Phys. Rev. B **48** *8952*
Ford W K, Guo T, Wan K-J and Duke C B 1992 *Phys. Rev.* B **45** 11896
Godby R W, Schlüter M and Sham L J 1988 *Phys. Rev.* B **37** 10159
Gonze X, Stumpf R and Scheffler M 1991 *Phys. Rev.* B **44** 8503
Heine V 1965 *Phys. Rev.* A **138** 1698
Hohenberg P Kohn W 1964 *Phys. Rev.* **136** B864
Huijser A, van Laar J and van Rooy T L 1977 *Surf. Sci.* **62** 472
Jenkins S J, Srivastava G P and Inkson J C 1993 *Phys. Rev.* B at press
Joyce J J, Nelson M M, Tang M, Meng Y, Anderson J and Lapeyre G J 1990 *J. Vac. Sci. Technol.* A **8** 3542
Kahn A 1983 *Surf. Sci. Rep.* **3** 193
Kendelewicz T, Woicik J C, Miyano K E, Herrera-Gomez A, Gowen P L, Karlin A, Bouldin C E, Pianetta P and Spicer W E 1992 *Phys. Rev.* B **46** 7276
Kleinman L and Bylander D M 1982 *Phys. Rev. Lett.* **48** 1425
Kohn W and Sham L J 1965 *Phys. Rev.* **140** A1133
LaFemina J P, Duke C B and Mailhiot C 1990 *J. Vac. Sci. Technol.* B **8** 888
Mailhiot C, Duke C B and Chadi D J 1985 *Phys. Rev.* B **31** 2213
Mårtensson P and Feenstra R M 1988 *J. Microsc.* **152** 761
—— 1989 *Phys. Rev.* B **39** 7744
Manghi F, Bertoni C M, Calandra C and Molinari E 1981 *Phys. Rev.* B **24** 6029
Manghi F, Calandra C and Molinari E 1987 *Surf. Sci.* **184** 449
Manghi F, Del Sole R, Selloni A and Molinari E 1990 *Phys. Rev.* B **41** 9935
Miyano K E, Cao R, Kendelewicz T, Wahi A K, Lindau I and Spicer W E 1990 *Phys. Scri.* **41** 973
Miyano K E, Kendelewicz, Woicik J C, Cowen P L, Bouldin C E, Karlin B A, Pianetta P and Spicer W E 1992 *Phys. Rev.* B **46** 6869
Miyano K E, Woicik J C, Kendelewicz T, Spicer W E, Richter M and Pianetta P 1993 *Phys. Rev.* B **47** 6444
Nannarone S, D'Addato S, Schaefer J A, Chen Y, Anderson J and Lapeyre G J 1989 *Surf. Sci.* **211/212** 524
Pauling L 1967 *The Nature of the Chemical Bond* (Ithaca, NY: Cornell University Press)
Payne M C, Joannopoulous J D, Allan D C, Teter M P and Vanderbilt D H 1986 *Phys. Rev. Lett.* **56** 2656
Payne M C, Teter M P, Allan D C, Arias T A and Joannopoulos 1992 *Rev. Mod. Phys.* **64** 1045
Perdew J P and A Zunger 1981 *Phys. Rev.* B **23** 5048
Phillips J C 1970 *Rev. Mod. Phys.* **42** 317
Riesterer T, Perfetti P, Tschudy M and Reihl B 1987 *Surf. Sci.* **189/190** 795
Skeath P, Su C Y, Harrison W A, Lindau I and Spicer W E 1983 *Phys. Rev.* B **27** 6246
Solal F, Jezequel G, Houzay F, Barski A and Pinchaux R 1984 Solid State Commun. **52** 37
Srivastava G P 1992 *Phys. Rev.* B **46** 7300
Srivastava G P and Martin R P 1992 *J. Phys.: Condens. Matter* **4** 2009
Srivastava G P, Singh I, Montgomeray V and Williams R H 1983 *J. Phys. C: Solid State Phys.* **16** 3627
Srivastava G P and Weaire D 1987 *Adv. Phys.* **36** 463
Straub D, Skibowski M and Himpsel F 1985 *J. Vac. Sci. Technol.* A **3** 1484
Stringer C, McKinley A, Hughes G and Williams R H 1983 *Vacuum* **33** 597
Swarts C A, Goddard W A and McGill T C 1982 *J. Vac. Sci. Technol.* **17** 982
Tulke A and Lüth H 1986 Surf. Sci. **178** *131*
van Laar J, Huijser A and van Rooy T L 1977 *J. Vac. Sci. Technol.* **14** 894
Yamamoto Y and Fujiwara T 1992 *Phys. Rev.* B **46** 13596
Zhu X, Zhang S B, Louie S G and Cohen M L 1989 *Phys. Rev. Lett.* **63** 2112